SCIENTIFIC BASIS OF INNOVATION

https://doi.org/10.15407/scine22.04.077

MORKUN, V. S. [1] (https://orcid.org/0000-0003-1506-9759),
MORKUN, N. V. [2] (https://orcid.org/0000-0002-1261-1170),
HRYSHCHENKO, S. M. [3] (https://orcid.org/0000-0003-4957-0904),
and HRYSHCHENKO, Ya. O. [4] (https://orcid.org/0009-0002-0582-4140)

[1] Kryvyi Rih National University,
11, Vitaliya Matusevycha St., Kryvyi Rih,
Dnipropetrovsk region, 50000, Ukraine,
+380 56 409 0606, knu@knu.edu.ua
[2] Ivan Franko National University of Lviv,
1, Universytetska St., Lviv, 79000, Ukraine,
+380 32 239 4122, webmaster@lnu.edu.ua
[3] State Tax University,
31, Universytetska St., Irpin, Kyiv region, 08200, Ukraine,
+380 44 363 2730, 11.02@dpu.edu.ua
[4] Volodymyr Dahl East Ukrainian National University,
17, John Paul II St., Kyiv, 01042, Ukraine,
+380 99 640 0286, vstup@snu.edu.ua

ENHANCEMENT OF FINE WET ORE SCREENING EFFICIENCY

Introduction. *Particle size classification of crushed ore is one of the key operations in the preparation of raw materials for metallurgical processing. The application of fine wet screening of ore pulp has enabled an increase in the concentration of valuable components in the processed products.*

Problem Statement. *The viscosity of ore pulp, caused by the presence of solid-phase particles and their aggregates of different sizes and densities, has reduced the rate at which particles pass through the screen apertures, thereby decreasing the efficiency of the screening process.*

Purpose. *To determine the effect of ultrasonic treatment on the dynamic viscosity of ore pulp and on the frictional interaction between crushed ore particles in order to improve the productivity and efficiency of fine wet screening.*

Materials and Methods. *The study has employed a combination of research methods, including the generalization of scientific information, analysis of particle interactions and acting forces during the screening process, mathematical and computer modeling, as well as experimental investigations.*

Citation: Morkun, V. S., Morkun, N. V., Hryshchenko, S. M., and Hryshchenko, Ya. O. (2026). Enhancement of Fine Wet Ore Screening Efficiency. *Sci. innov.*, 22(4), 77—89. https://doi.org/10.15407/scine22.04.077

© Publisher PH "Akademperiodyka" of the NAS of Ukraine, 2026. This is an open access article under the CC BY-NC-ND license (https://creativecommons.org/licenses/by-nc-nd/4.0/)

Results. *Under the influence of ultrasonic vibrations, additional forces have been generated in the ore pulp that act on solid-phase particles and gas bubbles. The most significant among them have been identified as the ultrasonic radiation pressure force and the pressure waves generated by cavitation collapse of gas bubbles. The obtained results have demonstrated that the application of ultrasonic treatment to the screen feed results in increasing the screening efficiency by 2—3%.*

Conclusions. *The proposed method for improving the efficiency of material separation by particle size, based on the introduction of ultrasonic vibrations of a specified amplitude and frequency into the feed material, has increased the mobility of crushed ore particles in the pulp, reduced interparticle adhesion forces, and created favorable conditions for cavitation effects and the destruction of heterophase aggregates. As a result, the quality of classification and the overall screening performance have been improved.*

Keywords: wet screening, vibrations, ultrasound, modeling, radiation pressure, cavitation.

The main goal of modern mineral processing technology is to achieve the highest possible productivity of the technological line while ensuring the appropriate quality of the final product, i.e. the content of a useful component in it should not be lower than the predefined level. At the same time, certain levels of energy efficiency and safe environmental impact must be achieved.

Size classification of crushed ore is one of the key aspects of its processing. In recent years, concentrators have increasingly used fine screens instead of the traditional mechanical hydraulic classifiers and hydrocyclones. The use of fine screening at low capital cost can increase the iron content of the concentrate by 1.7—2.7% in most operations [1, 2]. This is particularly important and relevant due to rising energy prices and increases in raw material and metallurgical production costs.

The input product for the fine screen is pulp, the concentration of the solid phase and the size of the ore particles in which depend on the stage of the benefaction process at which the corresponding operation of classifying the ore material by size takes place. The efficiency of the screening process can be determined by the following expression [3]:

$$\eta = \frac{m_{sp}}{m_{st}} \cdot 100\%, \qquad (1)$$

where m_{sp} is the total mass of sifted particles in the collection box under the sieve plate, the size of which is smaller than the sieve opening; m_{st} is the total mass of particles in the input product, the size of which is smaller than the sieve aperture.

From the above expression it is clear that this indicator depends on the characteristics of the pulp, the design features of the screen and the vibration parameters of the screen surface. In the process of screening, a layer of raw material is transported along the screen under the influence of the forces acting on it, and its particles, in contact with each other, move down to the screen surface, some of them pass through the screen and some remain on the surface. Thus, the efficiency and productivity of the screening process depends on how the contact interaction of the crushed ore particles on the screen surface occurs and how this process is affected by the forces acting on them.

The objective of the research is to determine the effect of ultrasound on the dynamic viscosity of iron ore pulp and the friction between the crushed ore particles in it, in order to increase the productivity and efficiency of the screening process.

Currently, there are many examples of the use of ultrasound to reduce the viscosity and internal friction of various products. In particular, the effect of ultrasonic irradiation time on the viscosity reduction of heavy oil is studied in [4]. The viscosity reduction rate (VRR) was determined using the formula:

$$VRR = \frac{\mu_o - \mu}{\mu_0} \cdot 100\%, \qquad (2)$$

where VRR is the viscosity reduction rate; μ_0(Pa · s) is the initial viscosity of the samples μ(Pa · s) is the viscosity at the end of of the ultrasound exposure.

It was determined that under the current experimental conditions, the VRR reached more than

80% and was best at an irradiation time of 6 minutes. When the irradiation time reached 12 minutes, the viscosity of the oil samples increased. Chemical analysis showed that the light components in the oil samples increased after ultrasonic irradiation, indicating that the cavitation, thermal and mechanical effects of ultrasound may play a role in breaking long carbon chains, thus reducing the viscosity. The increase in viscosity could be caused by reactivation between molecules and/or coking of the heavy oil.

The effect of ultrasound (US) on the shear viscosity of water soluble polymers has also been investigated [5]. Ultrasound with frequencies of 23, 43, 96, and 141 kHz and power of 8.5—9 W was used. The effect of ultrasound significantly reduced the shear viscosity of the solutions in the following order: 43 > 23 > 96 >141 kHz. After the ultrasound irradiation was stopped, the shear viscosity of aqueous polymer solutions returned to its original values. The ultrasonic stimulation was maintained during the experiments by controlling the ultrasonic power transmitted through the aqueous polymer solution. It was concluded that the ultrasonic irradiation affected the hydrogen bonding interaction between the OH groups of the polymer and the water molecules in the aqueous medium.

Similar results were obtained when studying the effect of ultrasonic waves at a frequency of 25 and 68 kHz and a power of 100, 250, and 500 W on the viscosity of paraffin, synthetic oil, and kerosene [6]. The experiments were performed under both controlled and uncontrolled temperature conditions in a smooth capillary tube. The results show that the viscosity of the liquids decreases under the influence of ultrasound, which may be due to the induced heat generation and cavitation in the liquid. The peculiarities of the influence of ultrasonic frequency, power and temperature on the viscosity reduction are discussed and interpreted.

In [7], the effect of solid fraction concentration, solid spherical particle diameter, suspended liquid viscosity and shear rate on suspension viscosity was experimentally investigated. It is shown that the suspension behavior can be well described by the Ostwald-de Weijle model, i.e. a power-law relationship between shear stress and shear rate. For low solid fraction concentration, the behavior is almost Newtonian, while with increasing solid fraction concentration, shear thinning is observed. For numerical evaluation of the results, the relative viscosity of the

$$\mu_{rel} = \frac{\mu_{sus}}{\mu_{liq}}, \quad (3)$$

where μ_{rel} is the relative viscosity; μ_{sus} is the dynamic viscosity of the suspension; μ_{liq} is the dynamic viscosity of the liquid.

It is proved that μ_{rel} is a rapidly increasing function of the solid fraction. It is also concluded that for suspensions based on a high viscosity liquid, the effect of particle size is small, while for suspensions with a low liquid viscosity, the viscosity of the suspension decreases slightly with increasing particle size. The relative viscosity is higher for systems based on low-viscosity liquids compared to systems with high liquid viscosity.

Paper [8] considers the classical problem of the effective viscosity of a Newtonian fluid with solid spherical particles. It has been stated that a simple approximation without interaction gives the effective viscosity coefficient for a suspension in the form

$$\frac{\mu}{\mu_0} = \left(1 - 2.5\phi\right)^{-1}, \quad (4)$$

where μ is the viscosity of the suspension; μ_0 is the viscosity of the forming liquid; ϕ is the volume fraction of particles in the suspension.

It is believed that expression (3) is more accurate than the commonly used one at much higher particle fractions μ:

$$\frac{\mu}{\mu_0} = 1 + 2.5\phi. \quad (5)$$

A method based on the use of ultrasonic vibration to reduce friction was used in [9] to improve the accuracy of viscosity measurement. The proposed electromagnetically rotating viscometer (EMS) allows measuring the viscosity of a sample a contactless manner. Although the device can measure

low viscosities of less than 10 mPa-s, which was difficult to achieve with conventional rotational viscometers, the accuracy was limited to 10% due to the detrimental effects of mechanical friction. The EMS system is equipped with piezoelectric actuators to excite ultrasonic vibrations in the sample cell, thereby reducing mechanical friction. A theory to describe the mechanical friction between the rotating probe and the oscillating substrate is also proposed and compared with experimental results.

Ultrasonic standing wave technology has been used to create a platform for particle manipulation in microfluidics. In [10], it was investigated how the viscoelasticity of the fluid and the formation of acoustic boundaries in microcavities affect the perturbations caused by ultrasound. These perturbations affect the acoustic energy density (AED) and consequently the dynamics of particle transport. The proposed approach combines theoretical, numerical and experimental methods for particles much smaller than the sound wavelength. This improved approach allows us to separate the AED and the acoustic contrast factor in expression (ARF). The influence of the viscoelastic parameters μ^* (the ratio of the viscosity of the viscoelastic fluid to the viscosity of the underlying Newtonian fluid) and De (the product of the fluid relaxation time and the activation frequency) on AED and particle migration is investigated. It is concluded that elastic effects accelerate particle migration while viscous effects slow it down. That is, particle migration can be controlled by adjusting viscoelastic and acoustic parameters at a fixed input power.

There are many examples of the successful use of ultrasound to reduce the viscosity of various products. The application of this approach in mineral processing operations is a promising way to increase their efficiency. However, the rationale for applying ultrasonic impact to iron ore pulp, which is a complex heterogeneous system containing crushed ore particles of different densities and sizes, gas bubbles and their various aggregations, requires additional research.

SUMMARY OF THE MAIN RESEARCH MATERIAL

In order to substantiate the increase in the efficiency of wet fine screening of ores by applying ultrasonic shock to them, the complex of force-contact interactions arising during the implementation of this process was studied.

The crushed ore particles are subjected to various and multidirectional forces during their movements in the pulp flow. The forces of hydrodynamic interaction for ore pulp with a high concentration of the solid phase include the Stokes drag force and the lubrication force, as well as the hydrodynamic force and torque acting on each particle α [11]:

$$F_\alpha^{(H)} = F_\alpha^{(S)} + \sum_{\beta\neq\alpha} F_{\alpha\beta}^{(L)}, \quad (6)$$

$$T_\alpha^{(H)} = T_\alpha^{(S)} + \sum_{\beta\neq\alpha} T_{\alpha\beta}^{(L)}, \quad (7)$$

where $F_\alpha^{(S)}$ is the Stokes drag force; $T_\alpha^{(S)}$ is the torque; $F_{\alpha\beta}^{(L)}$ is the lubrication force in the near zone; $T_{\alpha\beta}^{(L)}$ is the torque between particles α and β;

$$F_\alpha^{(S)} = U^\infty(r_\alpha) - U_\alpha, \quad (8)$$

$$T_\alpha^{(S)} = (4/3)\cdot(\Omega^\infty - \Omega_\alpha), \quad (9)$$

where r_α is the position of the particle; U_α is the translational velocity of the particle; Ω_α is the rotational velocity of the particle; U^∞ is the flow velocity.

The lubricating forces act only when the gap between the particle surfaces $h_{\alpha\beta} = r_{\alpha\beta} - 2$ satisfies the constraint $h_{\alpha\beta} \le 0.5$. Here, $r_{\alpha\beta}$ is the length of the vector $r_{\alpha\beta} = r_\beta - r_\alpha$, connecting particles α and β.

According to the Hertzian contact theory and the Mindlin-Deresiewicz contact theory [3, 12, 13], when two spherical particles with radii R_1 and R_2 are in contact, the normal contact force F_n, corresponding to the amount of overlap s in the normal direction, can be calculated by the following formula

$$F_n = \frac{4}{3} E^* \left(R^*\right)^{\frac{1}{2}} s^{\frac{3}{2}}, \quad (10)$$

where R^* and E^* are the equivalent radius and equivalent Young's modulus, respectively, calculated by the following formula

$$\frac{1}{R^*} = \frac{1}{R_1} + \frac{1}{R_2}, \quad (11)$$

$$\frac{1}{E^*}=\frac{1-\mu_1^{\ 2}}{E_1}+\frac{1-\mu_2^{\ 2}}{E_2}, \quad (12)$$

where E_1 and E_2 are the Young's modulus of spherical particles with radius R_1 and R_2 radius, respectively; μ_1 and μ_2 Poisson's ratio of spherical particles with radius R_1 and R_2 radius, respectively.

Equation (10) shows that at a time step, if the increment of overlap between two contacting particles is Δs, then the corresponding increment of normal contact force is ΔF_n:

$$\Delta F_n = 2aE^*\Delta s, \quad (13)$$

where $a=\sqrt{sR^*}$ is the contact radius.

In addition to the normal contact force, particles in contact under the conditions $h_{\alpha\beta} \le 2\in$ ($\in$ is the roughness of the particle) experience friction in the tangential direction [11, 14, 15]. According to Coulomb's law of friction, when two particles are in contact, the magnitude of the frictional force $F_{\alpha\beta}^{(C,t)}$ opposing their relative motion, taking into account (13), is equal to [11]:

$$F_{\alpha\beta}^{(C,t)}=\begin{cases}\mu F_{\alpha\beta}^{(C,t)}, \\ \text{if } \left|\Delta U_{\alpha\beta}^{(t)}\right|\neq 0 \text{ (dynamic mode)}, \\ 0\ldots\mu F_{\alpha\beta}^{(C,t)}, \\ \text{if } \left|\Delta U_{\alpha\beta}^{(t)}\right|=0 \text{ (dynamic mode)},\end{cases} \quad (14)$$

where μ is the friction coefficient; $\Delta U_{\alpha\beta}^{(t)}$ is the relative tangential velocity of the particle surfaces;

$$\Delta U_{\alpha\beta}^{(t)}=(I-n_{\alpha\beta}n_{\alpha\beta})\times \\ \times\left[U_\beta-U_\alpha-(\Omega_\alpha+\Omega_\beta)\cdot n_{\alpha\beta}\right], \quad (15)$$

where I is the identity tensor; $n_{\alpha\beta}=r_{\alpha\beta}/r_{\alpha\beta}$ is a unit vector directed from particle α to particle β.

The main statistical parameters describing the characteristics of the complex of contact interaction of crushed ore particles are the ratio of the power chain components and the contact angle [16].

The ratio of the components of the force chain quantitatively represents the general direction of expansion of the morphology of the force chain through the ratio of the components of the contact force in the direction of the x-axis and in the direction of the y-axis [17]. The calculation is as follows:

$$\mu_c=\frac{\sum_{i=1}^{n}f_i^y-\sum_{i=1}^{n}f_i^x}{\sum_{i=1}^{n}f_i^x+\sum_{i=1}^{n}f_i^y}, \quad (16)$$

where f_i^x is the value of the contact force component of contact i on the x-axis; f_i^y is the value of the contact force component of contact i on the y-axis; n is the total number of contacts; μ_c is the ratio of the force chain components (when; $\mu_c > 0$, the force chain is inclined to the vertical direction, i.e. the direction of the y-axis; when; $\mu_c < 0$, the force chain is inclined to the horizontal direction, i.e. the direction of the x-axis).

The directionality and local mechanical properties of the chain of forces are reflected in the statistical distribution of the contact angles of the particles and the average contact force. The formula for calculating the average contact force is as follows:

$$\overline{f}(\theta_c)=\frac{\sum_{i=1}^{N_c^k}F_i^k}{N_c^k}, \quad (17)$$

where θ_c is the angle between the normal and the horizontal of the contact plane, F_i^k is the contact force of the i-th contact in the k-th interval, N_c^k is the total number of contacts in the k-th interval, and $\overline{f}(\theta_c)$ is the average contact force (the greater the value of $\overline{f}(\theta_c)$, the greater the average contact force in the θ_c direction, and the greater the influence of the contact force on the stability of the system in the θ_c direction).

These parameters are used to quantitatively characterize the magnitude of the contact force, distribution concentration, shape and direction of the force chain.

Under the influence of ultrasonic vibrations in the ore slurry, forces act on solid phase particles and gas bubbles. The most influential of these are the radiation pressure force and the pressure wave resulting from the cavitation collapse of gas bubbles.

The radiation pressure force can be represented by the scattering σ_s and absorption σ_p cross sections of the ultrasonic wave on the particles [18]:

$$F_r = \frac{I}{c}(\sigma_p + \sigma_s \mu), \quad (18)$$

where I is the intensity of the incident wave; c is its propagation velocity;

$$\mu = \frac{2\pi}{\sigma_s}\int_{-1}^{1} d\cos\nu \frac{d\sigma}{d\Omega}(\cos\nu)\cdot(1-\cos\nu).$$

For spherical particles of radius r, the differential effective scattering cross section is given by

$$\frac{d\sigma}{d\Omega}(\cos\nu) = \frac{r^2}{9}(kr)^4\left(a_1 - \frac{3}{2}a_2\cos\nu\right)^2, \quad (19)$$

where $a_1 = 1-(rc^2/\rho_T c_T^2)$, $a_2 = 2(\rho_T - \rho/2\rho_T + \rho)$, ρ_T, c_T are the density and ultrasound velocity in the particle material, respectively; ρ is the density of the medium.

The nature of the change in the concentration of particles and their size distribution in the ultrasound field depends on the density of the particles themselves, the frequency and intensity of the radiation affecting them. Let us estimate the effect of ultrasonic radiation pressure on the change in the concentration of particles of radius r. Let the pulp flow in the positive direction of the x-axis with a velocity V. Let $n_r(Z, t)$ denote the concentration of particles of radius r at depth Z at time t. Taking into account the above, we can write:

$$\frac{\partial n_r(Z,t)}{\partial t} = -\frac{\partial}{\partial Z}\left[V_r(Z,t)\, n_r(Z,t)\right]. \quad (20)$$

In this equation, $V_r(Z, t)$ is the velocity of displacement of a particle of radius r with coordinate Z by the ultrasonic field. The velocity is directed along the z-axis, i.e. perpendicular to the pulp flow. In general, it depends on time t, because as a result of ultrasound, the particle concentration changes, and this leads to a change in ultrasound intensity, which ultimately affects the particle displacement rate. However, this greatly complicates the solution of equation (20), so we will assume that the velocity depends only on the Z coordinate.

Assuming that the intensity of the ultrasonic wave I changes according to an exponential law (initial value I_0), its attenuation coefficient α depends on the sound frequency ν_0 and taking into account the analysis performed in [18, 23], the particle concentration $n_r(Z, t)$ is determined by the formula

$$n_r(Z,t) = n_0 \frac{e^{\alpha z}}{e^{\alpha z} - \alpha\beta t} St(e^{\alpha z} - 1 - \alpha\beta t), \quad (21)$$

where $n_r(Z, 0) = n_0$, $n_r(0, t) = 0$ are the initial and boundary conditions; c is the ultrasonic speed in the medium;

$$St(X) = \begin{cases} 0, & X < 0 \\ 1, & X \geq 0 \end{cases};$$

$$\beta = \frac{2r(kr)^4}{27\eta c} I_0\left(a_1^2 + a_1 a_2 + \frac{3}{4}a_2^2\right);$$

$$a_1 = 1 - \frac{rc^2}{\rho_T c_T^2}; \quad a_2 = 2\frac{\rho_T - \rho}{2\rho_T + \rho}.$$

The mechanism of ultrasound propagation in the gas phase of a pulp differs significantly from that in the solid phase. The gas bubbles oscillate in phase with the applied ultrasonic wave, shrinking under compression and expanding under rarefaction. The resonance size of the gas bubble depends on the applied ultrasonic field frequency. When the resonant size is reached, due to growth by rectified diffusion or coalescence, either transient (inertial) cavitation can occur, where the bubble becomes unstable and collapses within one or several acoustic cycles, or steady cavitation, where the bubble oscillates for many cycles near the linear resonant size.

Phenomena such as the heating of the bubble, periodic changes in its volume that it undergoes under the action of a sound wave, dissipation of part of the acoustic energy due to the fact that the bubble is a spherical sound radiator, heat transfer to the liquid, as well as energy losses due to the formation of liquid currents around the bubble explain the fact that bubbles with dimensions close to the resonance size cause significant attenuation of the sound energy.

To account for the gas pressure in the bubble and the changing pressure in the liquid, as well as viscosity and surface tension, it is advisable to use

the Rayleigh-Plesset equation of cavitation bubble dynamics [24, 25]:

$$\frac{P_L - P_\infty}{\rho} = R\ddot{R} + \frac{3}{2}\dot{R}^2, \quad (22)$$

where R is the radius of the bubble, $\dot{R}$ is the wall velocity, P_∞ is the pressure in the liquid at infinity, P_L is the pressure in the liquid at the bubble wall, and ρ is the density of the liquid.

Taking into account the effects of the surface viscosity of the fluid, tension, and Laplace pressure, at $R = R_0$ and the gas pressure in the bubble $P_0 + 2\sigma/R_0$, the equation can be expressed as follows [26, 27]:

$$R\ddot{R} + \frac{3}{2}\dot{R}^2 = \frac{1}{\rho} \times$$

$$\times \left[\left(P_0 + \frac{2\sigma}{R_0} \right) \left(\frac{R_0}{R} \right)^{3\gamma} - \frac{2\sigma}{R} - \frac{4\mu\dot{R}}{R} + P_\infty \right], \quad (23)$$

where P_0 is the static pressure in the liquid, σ is the surface tension, μ is the viscosity of the liquid.

As a result of the impact of ultrasound on gas bubbles, the pressure P changes according to the following law:

$$P = P_0 - P_A \sin \omega t, \quad (24)$$

where P_0 is the constant pressure, ω is the angular frequency, and P_A is the amplitude of the excitation pressure.

The cavitation collapse of a gas bubble is a particularly important event because of the consequences that can be caused by the high velocities, pressures and temperatures that result from this event [28].

Thus, the irradiation of the ore pulp with ultrasound is accompanied by the absorption and dissipation of acoustic energy, creating a dynamic impact and the potential to generate shock waves, high pressures and temperatures during the collapse of gas bubbles. These phenomena, in turn, contribute to the reduction of contact interaction between ore particles and the destruction of their aggregations and flocculations.

In accordance with the above equations and using scenarios and tools [29, 31], the dynamics of a gas bubble in the ultrasonic impact field has been calculated. The obtained results show that the cavitation bubble nucleus expands rapidly in the ultrasound-induced pressure field, the pressure wave is emitted and propagates in the liquid during the subsequent bubble collapse. When the pressure wave collides with an obstacle, it causes a high pressure peak on the surface of the obstacle, which contributes to its destruction [32].

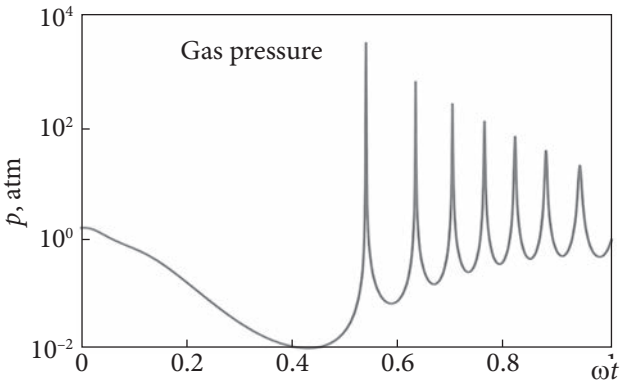


Fig. 1. Pressure change during cavitation collapse of a gas bubble

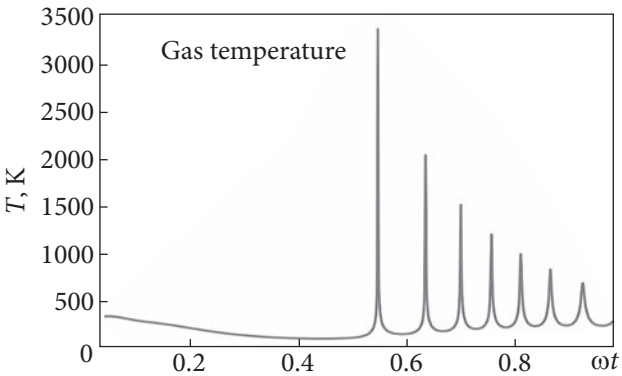


Fig. 2. Temperature change during the cavitation collapse of a gas bubble

Figure 1 shows changes in gas pressure, while Fig. 2 features changes in temperature during the collapse of a gas bubble (the primary radius of the bubble is 10 μm, the frequency the acoustic impact is 21.5 kHz).

When a cavitation bubble grows from a small nucleus to many times its initial size, collapse begins at the maximum radius (37 μm in the example above) at a very low partial pressure of the gas

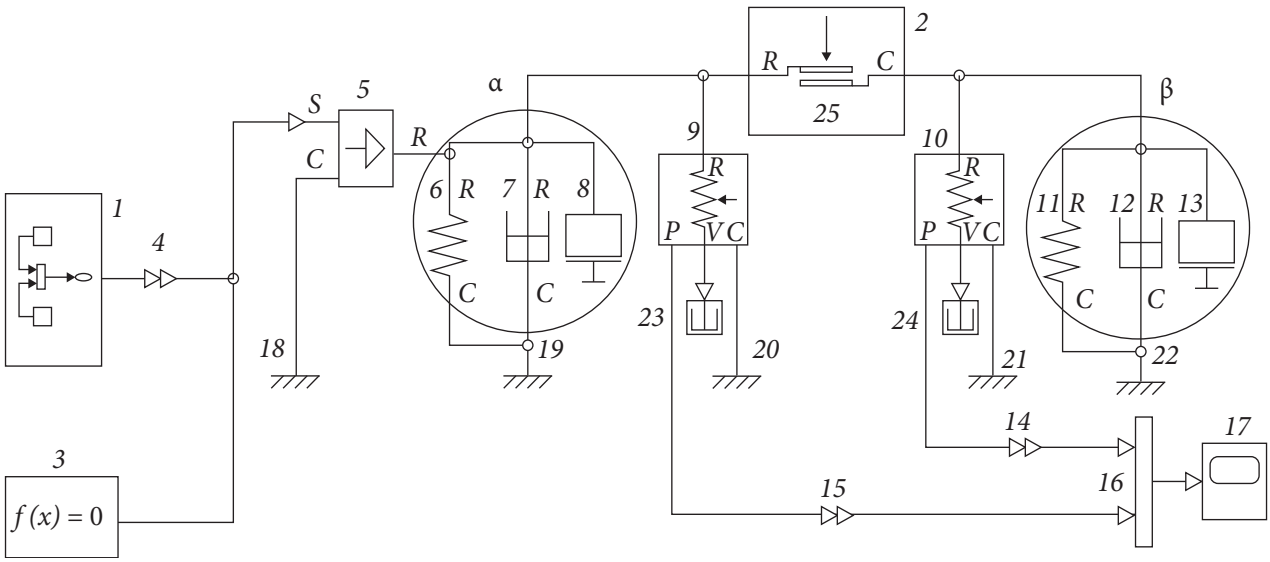


Fig. 3. Scheme of the modeling of the ultrasonic effect on the interaction of crushed ore particles in the pulp

(0.0046 atm). In the example shown in Figs. 1, 2, the peak pressure value is 5420 atm and the temperature is 3310 K, which is many times higher than the ambient temperature.

Many factors, including the characteristics of the solid and gas phases in the pulp flow and the above factors of interaction of its components, affect this result.

The modeling of the contact interaction of the crushed ore particles under the influence of high-energy ultrasound, taking into account the above factors, was carried out in the Simscape/Simulink Matlab extension. A generalized scheme of the model is shown in Fig. 3.

In the model shown in Fig. 3 of the model used the following blocks of the corresponding Simscape® extension libraries for Simulink® /MATLAB® [28]: *1* — Subsystem for forming the parameters of the mechanical impact signal; *2* — Subsystem for forming the parameters of the ultrasonic impact; *3* — Solver Configuration block; *4* — Simulink — PS Converter block; *5* — Ideal Translational Velocity Source block; *6, 11* — Translational Spring block; *7, 12* — Translational Damper block; *8, 13* — Mass block; *9, 10* — Ideal Translational Motion Sensor block; *14, 15* — PS—Simulink Converter block; *16* — Mux block; *17* — Scope block; *18*—*22* — Mechanical Translational Reference block; *23, 24* — PS Terminator block; *25* — Translational Friction block.

Subsystem for generating parameters of the mechanical disturbance signal *1* — generates electrical pulses of the selected shape, amplitude and duration and adds to them a signal simulating disturbances and interferences. Ideal Translational Velocity Source *5* is an ideal velocity source that generates at its terminals a velocity difference proportional to the input physical signal. The blocks contained in the structures labeled α and β simulate the elastic properties of ore particles. The velocity and displacement of the particles are measured by sensors *9, 10* and displayed by the Scope *17* block. The Solver Configuration block defines the solver parameters required by the model before starting the simulation.

The subsystem for the formation of ultrasonic impact parameters *2* is performed using the Translational Friction *25* block. This block models friction in contact between moving bodies. The friction force is modeled as a function of the relative velocity and is considered to be the sum of the Stribeck, Coulomb and viscosity components.

Stribeck friction T_S is a characteristic with a negative slope that occurs at low speeds [34]. Coulomb friction T_C results in a constant torque at any speed. Viscous friction T_V opposes motion with a torque directly proportional to the relative speed. The sum of Coulomb and Stribeck friction in the vicinity of zero speed determines the breakaway friction T_{brk}. In general, rotational friction is approximated by the following equations [34]:

$$T = \sqrt{2e}\left(T_{brk} - T_C\right)\exp\left(-\left(\frac{w}{w_{St}}\right)^2\right)\cdot\frac{w}{w_{St}} + \\ + T_C \cdot \tanh\left(\frac{w}{w_{Coul}}\right) + fw, \quad (25)$$

where $w_{St} = w_{brk}\sqrt{2}$; $w_{Coul} = w_{brk}/10$; $w = w_R - w_C$; T is the friction moment; T_C is the Coulomb friction moment; T_{brk} is the breakaway friction moment; w_{brk} is the breakaway friction velocity; w_{St} is the Stribeck velocity threshold; w_{Coul} is the threshold of Coulombic velocity; w_R and w_C are the absolute angular velocities of ports R and C of the rotational friction unit; ω is the relative velocity; f is the coefficient of viscous friction.

The simulation of the effect of ultrasound on the variable parameters of the translational friction block is performed programmatically and in the Matlab command window.

Figure 4 shows the results of modeling the displacement of an ore particle β relative to a particle α in time from the applied ultrasonic impact of different power with a frequency of 21.5 kHz.

The obtained results show that the applied ultrasonic impact on the ore particles in the pulp flow leads to a decrease in their contact adhesion forces and, accordingly, contributes to an increase in the feed rate of the screened material.

The model shown in Fig. 3 was used to study the effect of ultrasonics on the efficiency of wet fine screening of ore pulp. The simulation results were compared with data obtained from the experimental setup, which fully reproduced the screening process on a reduced scale. The ultrasonic shock was generated by a piezoelectric transducer using phased array technology. The fundamental frequency of the transducer was 21.5 kHz, and the power of the generated signal was adjustable in the range of 0—150 W. The generated signal was injected into the incoming pulp stream on the screen. The screening efficiency was evaluated by standard laboratory methods according to expression (1).

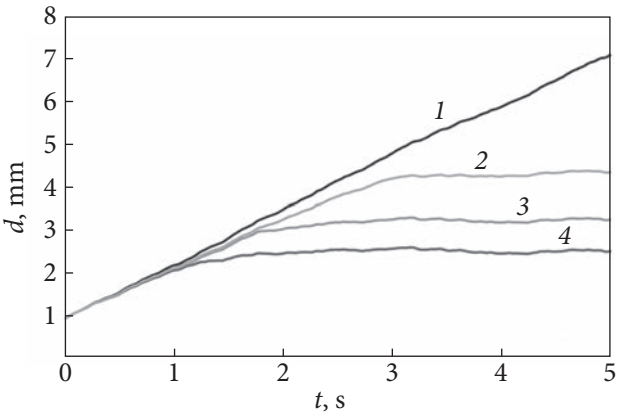


Fig. 4. Results of modeling the effect of ultrasound on the displacement of ore particle 4 relative to particle 3: *1* — displacement of particle α; *2* — displacement of particle β, ultrasound power P_1 = 100 W; *3* — displacement of particle β, ultrasound power P_2 = 125 W; *4* — displacement of particle β, ultrasound power P_3 = 150 W

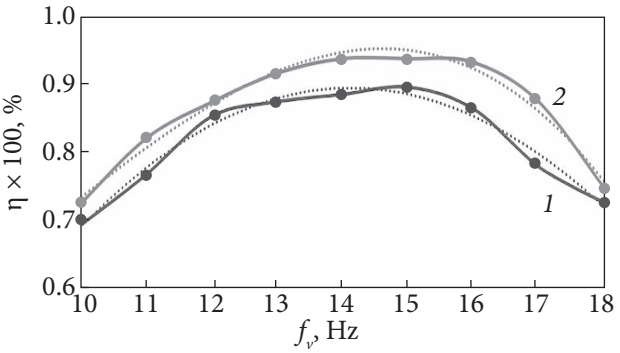


Fig. 5. The results of ultrasonic influence on the process of wet fine screening of ore: *1* — without ultrasonic irradiation; *2* — with ultrasonic irradiation

The effect of ultrasonic irradiation of the pulp on the screening efficiency in conventional screen operating modes was investigated. Figure 5 shows

the results of screening ore pulp with a density of 1.600 g/cm^3 and a size of 85% of the — 74 μm class on a screen whose operating vibration frequency varied within 10—18 Hz.

The dependencies shown in Fig. 4 are approximated by the following expressions:

$$y_1 = -0.0008x^3 + 0.0222x^2 - \\ -0.1296x + 0.6224,\ R^2 = 0.9829, \quad (26)$$

$$y_2 = 3 \cdot 10^{-5}x^3 - 0.0126x^2 + \\ +0.335x - 1.4293,\ R^2 = 0.9781. \quad (27)$$

The results obtained indicate that the added ultrasonic effect on the input product of the screen, within the limits of technological changes in its density and particle size distribution and taking into account additional energy costs, increases the efficiency of the process by 2—3%. Another positive result of the proposed approach is the improvement of the conditions for maintaining the cleanliness of the screen surface holes by reducing ore aggregation and flocculation in the pulp. This also increases the contrast of the products obtained for further magnetic separation and flotation operations.

The complex of force-contact interactions arising during the implementation of the process of fine wet screening of ores has been studied. Under the influence of ultrasonic vibrations in the ore pulp, forces acting on the particles of the solid phase and gas bubbles are created. The most influential of them are the force of ultrasonic radiation pressure and the pressure wave resulting from cavitation collapse of gas bubbles.

A method for increasing the efficiency of particle-size separation of screened material has been proposed. According to this method ultrasonic vibrations of a specified amplitude and frequency have been introduced into the feed material. This approach has enabled an increase in the mobility of crushed ore particles within the pulp, a reduction in interparticle contact adhesion forces, and the creation of conditions for cavitation effects in gas bubbles and the destruction of heterophase aggregates, thereby improving the quality of classification and the overall screening performance.

The modeling and experimental investigations have demonstrated that the application of ultrasonic treatment to the screen feed has resulted in increasing the efficiency of the process by 2—3%.

This research is funded by the Alexander von Humboldt Foundation.

REFERENCES

1. Bulakh, O. V. (2017). Determination of the feasibility of using a fine screening operation in the beneficiation of magnetite quartzite. *Mineral processing*, 67(108). URL: http://zzkk.nmu.org.ua/pdf/2017-67-108/08.pdf (Last accessed: 03.04.2026).
2. Oliynyk, T. A., Sklyar, L. V., Oliynyk, M. O., Kushniruk, N. V., Sklyar, A. Y., Korzhan, I. A. (2018). The use of fine screening in the conditions of PJSC Northern GOK. *Mineral processing*, 69(110), 69—77. URL: http://zzkk.nmu.org.ua/pdf/2018-69-110/9.pdf (Last accessed: 03.04.2026).
3. Chen, B., Yan, J., Mo, W., Xu, C., Zhang, L., Tamma Kumar, K. (2019). DEM simulation and experimental study on the screening process of elliptical vibration mechanical systems. *Journal of vibroengineering*, 21(8), 2025—2038. https://doi.org/10.21595/jve.2019.19993
4. Gao, J., Li, C., Xu, D., Wu, P., Lin, W., Wang, X. (2021). The mechanism of ultrasonic irradiation effect on viscosity variations of heavy crude oil. *Ultrasonics Sonochemistry*, 81, 105842. https://doi.org/10.1016/j.ultsonch.2021.105842
5. Venegas-Sanchez, J., Tagaya, M., Kobayashi, T. (2013). Effect of ultrasound on the aqueous viscosity of several water-soluble polymers. *Polymer journal,* 45, 1224—1233. https://doi.org/10.1038/pj.2013.47
6. Hamidi, H., Mohammadian, E., Junin, R., Rafati, R., Azdarpour, A., Junid, M., Savory, R. M. (2014). The Effect of Ultrasonic Waves on Oil Viscosity. *Petroleum Science and Technology*, 32, 2387—2395. https://doi.org/10.1080/10916466.2013.831873

7. Konijn, B. J., Sanderink, O. B. J, Kruyt, N. P. (2014). Experimental study of the viscosity of suspensions: Effect of solid fraction, particle size and suspending liquid. *Powder Technology*, 266, 61—69. https://doi.org/10.1016/j.powtec.2014.05.044
8. Abedian, B., Kachanov, M. (2010). On the effective viscosity of suspensions. International *Journal of Engineering Science,* 48(11), 962—965. https://doi.org/10.1016/j.ijengsci.2010.08.012
9. Matsuura, Y., Hirano, T., Sakai, K. (2014). Friction torque reduction by ultrasonic vibration and its application to electromagnetically spinning viscometer. *Japanese Journal of Applied Physics*, 53(7S). https://doi.org/10.7567/JJAP.53.07KC12
10. Sujith, T., Malik, L., Sen, A. K. (2024). Fluid viscoelasticity affects ultrasound force field-induced particle transport. *Journal of Fluid Mechanics,* 1000, A75. https://doi.org/10.1017/jfm.2024.965
11. Zhang, H., Kopelevich, D. I., Butler, J. E. (2024). Frictional effects on shear-induced diffusion in suspensions of non-Brownian particles. *Journal of Fluid Mechanics*, 1001, A42. https://doi.org/10.1017/jfm.2024.1121
12. Zhou, Z. Y., Kuang, S. B., Chu, K. W., Yu, A. B. (2010). Discrete particle simulation of particle–fluid flow: model formulations and their applicability. *Journal of Fluid Mechanics,* 661, 482—510. https://doi.org/10.1017/S002211201000306X
13. Dong, K. J., Yu, A. B. (2012). Numerical simulation of the particle flow and sieving behaviour on sieve bend/low head screen combination. *Minerals Engineering*, 31(4), 2—9. https://doi.org/10.1016/j.mineng.2011.10.020
14. Thorsten, Pöschel, Schwager, T. (2005). *Computational Granular Dynamics: Models and Algorithms.* Springer Science & Business Media.
15. Radjai, F., Dubois, F. (2011). *Discrete-element modeling of granular materials.* Wiley-Iste.
16. Chen, Q., Qin, S., Wu, S. (2020). Quantitative Study on the Contact Force and Force Chain Characteristics of Ore Particle Systems during Ore Drawing from a Single Drawpoint under the Influence of a Flexible Barrier. *Hindawi, Geofluids*, 1270761, 13. https://doi.org/10.1155/2020/1270761
17. Zhang, W., Zhou, J., Yu, S. W., Zhang, X., Liu, K. (2018). Quantitative investigation on force chains of metal powder in high velocity compaction by using discrete element method, *Journal of Mechanical Engineering*, 54(10), 85—92. https://doi.org/10.3901/JME.2018.10.085
18. Morkun, V. S., Potapov, V. M., Morkun, N. V., Podgorodetsky, M. S. (2007). *Ultrasonic control of the characteristics of crushed materials in the process control system of the beneficiation production.* Kryvyi Rih.
19. Xu, N., Tang, S., Lin, D., Geng, R., Wang, X., Liang, X. (2024). Complex granular flows of sticky-wet material on flip-flow screens: Calibration of discrete element simulations. *Particuology*, 84, 290—308. https://doi.org/10.1016/j.partic.2023.07.010
20. Wang, S., Wang, X. Fucheng, You, Han, Xiao. (2023). Review of Ultrasonic Particle Manipulation Techniques: Applications and Research Advances. *Micromachines,* 14(8), 1487. https://doi.org/10.3390/mi14081487
21. Zhang, W., Zhou, J., Yu, S. W., Zhang, X. J., Liu, K. (2018). Investigation on contact force and force chain of granular matter in biaxial compression. *Chinese Journal of Applied Mechanics*, 35, 530—538.
22. Yang, G., Lin, W., Lai, H., Tong, J., Lei, J., Yuan, M., Zhang, Yu., Cui, C. (2021). Understanding the relationship between particle size and ultrasonic treatment during the synthesis of metal nanoparticles. *Ultrasonics Sonochemistry*, 73, 105497. https://doi.org/10.1016/j.ultsonch.2021.105497
23. Morkun, V., Morkun, N., Tron, V., Hryshchenko, S., Serdyu, O., Dotsenko, I. (2019). Basic regularities of assessing ore pulp parameters in gravity settling of solid phase particles based on ultrasonic measurements. *Archives of Acoustics*, 44(1), 161—167. https:// doi.org/10.24425/aoa.2019.126362
24. Noltingk, B. E., Neppiras, E. A. (1950). Cavitation produced by ultrasonics. *Proceedings of the Physical Society*, 63(9), 674. https://doi.org/10.1088/0370-1301/63/9/305
25. Morkun, V. S., Pikilnyak, A. V. (2017). *Adaptive control of the iron ore flotation process*. Kryvyi Rih.
26. Neppiras, E. A., Noltingk, B. E. (1951). Cavitation Produced by Ultrasonics: Theoretical Conditions for the Onset of Cavitation, *Proceedings of the Physical Society*, 64(12), 1032. https://doi.org/10.1088/0370-1301/64/12/302

27. Morkun, V., Morkun, N., Pikilnyak, A. (2017). Ultrasonic facilities complex for grinding and ore classification process control. *2017 IEEE 37th International Conference on Electronics and Nanotechnology* (*ELNANO*) (*18—20 April 2017, Kyiv*), 409—413, 7939788. https:// doi.org/10.1109/ELNANO.2017.7939788
28. Brennen, C. E. (1995). *Cavitation and Bubble Dynamics*. Oxford University Press. https://doi.org/10.1017/CBO9781107338760
29. Oncotripsy. URL: https://github.com/drmittelstein. (Last accessed: 20.09.2024).
30. Chen, Yue-han, Zhan, Jie-min, Li, Yu-tian. (2021). Numerical simulation of cavitation-bubble expansion and collapse inside a bottle subjected to impact on its topside. *Engineering Applications of Computational Fluid Mechanics,* 15(1), 1440—1451. https://doi.org/10.1080/19942060.2021.1976279
31. Johansen, K., Song, J. H., Prentice, P. (2017). Validity of the Keller-Miksis equation for "non-stable" cavitation and the acoustic emissions generated. *2017 IEEE International Ultrasonics Symposium* (*Ius*). https://doi.org/10.1109/ULTSYM.2017.8092224
32. Simscape. Model and simulate multidomain physical systems. URL: https://www.mathworks.com/products/simscape.html. (Last accessed: 20.09.2024).
33. Armstrong, B., de Wit, C.C. (1995). *Friction Modeling and Compensation*. The Control Handbook, CRC Press. Phd (tech). Lausanne.
34. Mechanical Rotational System with Stick-Slip Motion. URL: https://www.mathworks.com/help/simscape/ug/mechanical-rotational-system-with-stick-slip-motion.html (Last accessed: 20.11.2024).

Received 21.02.2025
Revised 11.01.2026
Accepted 03.02.2026

В.С. Моркун [1] (https://orcid.org/0000-0003-1506-9759),
Н.В. Моркун [2] (https://orcid.org/0000-0002-1261-1170),
С.М. Грищенко [3] (https:/orcid.org/0000-0003-4957-0904),
Я.О. Грищенко [4] (https://orcid.org/0009-0002-0582-4140)

[1] Криворізький національний університет,
вул. Віталія Матусевича, 11, Кривий Ріг,
Дніпропетровська область, 50000, Україна,
+380 56 409 0606, knu@knu.edu.ua
[2] Львівський національний університет імені Івана Франка,
вул. Університетська, 1, Львів, 79000, Україна,
+380 32 239 4122, webmaster@lnu.edu.ua
[3] Державний податковий університет,
вул. Університетська, 31, Ірпінь, Київська область, 08200, Україна,
+380 44 363 2730, 11.02@dpu.edu.ua
[4] Східноукраїнський національний університет імені Володимира Даля,
вул. Іоанна Павла II, 17, Київ, 01042, Україна,
+380 99 640 0286, vstup@snu.edu.ua

ПІДВИЩЕННЯ ЕФЕКТИВНОСТІ ТОНКОГО ВОЛОГОГО ГРОХОЧЕННЯ РУДИ

Вступ. Класифікація подрібненої руди за крупністю є одною з головних операцій у процесі її підготовки до металургійного переділу. Використання тонкого вологого грохочення рудної пульпи дозволяє підвищити вміст корисного компоненту у продуктах збагачення.

Проблематика. В'язкість пульпи, яка обумовлена наявністю в ній частинок твердої фази та їхніх агрегацій різної крупності й щільності, призводить до уповільнення процесу їх проходження через отвори сита.

Мета. Визначити вплив ультразвуку на динамічну в'язкість рудної пульпи та тертя між частинками подрібненої руди в ній для підвищення продуктивності й ефективності процесу грохочення.

Матеріали й методи. Застосовано комплекс методів досліджень, зокрема: узагальнення наукової інформації, аналіз взаємодії частинок руди у процесі грохочення та діючих на них сил, математичне та комп'ютерне моделювання процесів, експериментальні випробування.

Результати. Під впливом ультразвукових коливань у рудній пульпі виникають сили, що діють на частинки твердої фази та газові бульбашки. Найбільш впливовими з них є сила радіаційного тиску ультразвуку та хвиля тиску, що виникає при кавітаційному колапсі газових бульбашок. Отримані результати свідчать про те, що доданий ультразвуковий вплив на вхідний продукт грохота підвищує ефективність процесу на 2—3 %.

Висновки. Запропонований метод підвищення ефективності розділення на грохоті просіюваного матеріалу за крупністю його часток, за яким у вхідний продукт вводяться ультразвукові коливання певної амплітуди і частоти, дозволяє збільшити рухомість часток подрібненої руди у пульпі, зменшити сили їх контактного зчеплення, сформувати умови для проявлення кавітаційних ефектів у газових бульбашках та руйнування гетерофазних агрегацій, що спричиняє підвищення якості класифікації та продуктивність грохочення.

Ключові слова: вологе грохочення, вібрації, ультразвук, моделювання, радіаційний тиск, кавітація.